JACS
JOURNAL OF THE AMERICAN CHEMICAL SOCIETY
Article
pubs.acs.org/JACS

Charge Carrier Generation and Transport in Different Stoichiometry APFO3:PC61BM Solar Cells

Vytenis Pranculis,[†] Yingyot Infahsaeng,[‡] Zheng Tang,[§] Andrius Devižis,[†] Dimali A. Vithanage,[‡] Carlito S. Ponseca, Jr.,[‡] Olle Inganäs,[§] Arkady P. Yartsev,[‡] Vidmantas Gulbinas,[†] and Villy Sundström*[,‡]

[†]Center for Physical Sciences and Technology, Savanoriu 231, LT-02300 Vilnius, Lithuania

[‡]Division of Chemical Physics, Lund University, Box 124, 221 00 Lund, Sweden

[§]Biomolecular and Organic Electronics, Department of Physics (IFM), Linköpings University, SE-58183 Linköping, Sweden

ABSTRACT: In this paper we studied carrier drift dynamics in APFO3:$PC_{61}BM$ solar cells of varied stoichiometry (2:1, 1:1, and 1:4 APFO3:$PC_{61}BM$) over a wide time range, from subpicoseconds to microseconds with a combination of ultrafast optical electric field probing and conventional transient integrated photocurrent techniques. Carrier drift and extraction dynamics are strongly stoichiometry dependent: the speed of electron or hole drift increases with higher concentration of $PC_{61}BM$ or polymer, respectively. The electron extraction from a sample with 80% $PC_{61}BM$ takes place during hundreds of picoseconds, but slows down to sub-microseconds in a sample with 33% $PC_{61}BM$. The hole extraction is less stoichiometry dependent: it varies form sub-nanoseconds to tens of nanoseconds when the $PC_{61}BM$ concentration changes from 33% to 80%. The electron extraction rate correlates with the conversion efficiency of solar cells, leading to the conclusion that fast electron motion is essential for efficient charge carrier separation preventing their geminate recombination.

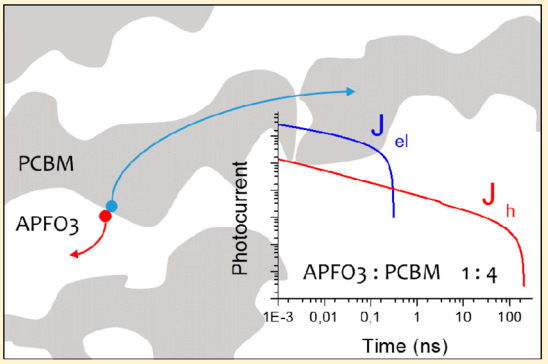

INTRODUCTION

The bulk heterojunction (BHJ) is currently a leading architecture of organic solar cells enabling successful combination of small exciton diffusion radius with much larger light absorption depth. Efficiencies of the best solar cells based on blends of various electron donating materials and fullerene derivatives have just reached 10%.[1,2] In efficient such devices, electron−hole pairs (CT states) formed through absorption overcome the electrostatic interaction and carriers escape from each other before they recombine. The escape appears to be governed by the properties of the initially formed electron−hole pair[3−5] and carrier drift and diffusion.[4,6,7] Delocalization of the hole in the polymer[4,5] or electron in the fullerene acceptor phase[3] could control the electron−hole binding energy. We have recently demonstrated that the carrier diffusion is mainly responsible for their separation at short times and short distances in BHJ solar cells, where the internal electric field is weak (or even nearly absent at flat band conditions).[6] Both electron and hole are mobile, therefore motions of both of them determine the carrier separation rate and distance. If their mobilities are very different, the separation would rely on motion of the faster one. The ability of holes to rapidly move through conjugated polymer chains was believed to be one of the major advantages of conjugated polymers over small molecules for their use in BHJ solar cells. However, efficiencies of solar cells based on various polymers and on small molecules are surprisingly similar, suggesting that polymer conjugation may not be that crucial for good solar cell performance. This leads to the conclusion that the large charge delocalization in conjugated polymers, which was previously believed to be of major importance for the charge carrier photogeneration, may not play a dominant role. On the other hand, attempts to substitute fullerene derivatives with other electron accepting molecules have been less successful. Moreover, high efficiency solar cells need a high fullerene content of 50% or more, significantly exceeding percolation threshold for the electron motion.[8] Many factors, such as dielectric permittivity, phase segregation, morphology, positions of electronic levels, etc., may play an important role[9−11] for the performance, but the electron mobility in the fullerene phase is apparently among the most important.

Carrier mobilities in conjugated polymers and fullerenes have been widely investigated. Stationary hole mobilities in conjugated polymers are of the order of 10^{-4}−10^{-6} $cm^2/(V\ s)$, but it was also demonstrated that the mobilities are orders of magnitude higher on short time and distance scales before carriers relax within the distributed density of states (DOS).[12,13] Apparently, those high initial mobilities are important for understanding charge carrier separation occurring on the picosecond and nanosecond time scales. Macroscopic electron mobilities in PCBM are higher, reported to be of the order of 10^{-2}−10^{-1} $cm^2/(V\ s)$.[14−18] Also electron mobilities were reported to be strongly time dependent.[19] Mobilities

Received: April 2, 2014
Published: July 15, 2014

   dx.doi.org/10.1021/ja503301m | J. Am. Chem. Soc. 2014, 136, 11331−11338

Table 1. Photovoltaic Performance Parameters and Modeled Mobility Parameters of Different Devices

device	J_{sc} (mA/cm^2)	V_{oc} (V)	FF	PCE (%)	modeled mobility [μ_0 (cm^2 V^{-1} s^{-1}), α]	
					electron	hole
neat APFO3	0.0998	0.757	0.243	0.0183	1.1×10^{-5}, 0.25	5.5×10^{-6}, 0.2
2:1	2.28	0.818	0.355	0.662	8×10^{-9}, 0.5	4×10^{-6}, 0.25
1:1	4.28	0.894	0.318	1.22	2.5×10^{-6}, 0.35	4.3×10^{-9}, 0.6
1:4	4.91	0.878	0.374	1.61	4.5×10^{-5}, 0.3	3.8×10^{-8}, 0.45
neat $PC_{61}BM$	0.171	0.301	0.40	0.021		

determined for neat materials may be significantly different from those in BHJ blends, because of different molecule packing and of boundaries between polymer and fullerene domains, which may create major obstacles for the carrier motion. The relative magnitude of electron and hole mobilities on short time and distance scales in various polymer/fullerene blends is therefore not known in general, as is their importance for generation of free charges and their extraction.

In this paper we address this issue in APFO3:$PC_{61}BM$ blends by using ultrafast optical probing of the intrinsic electric field by time-resolved electric field-induced second harmonic generation (TREFISH) measurements, combined with conventional transient integrated photocurrent measurements. This enables us to monitor charge generation, separation, and extraction from the sample over the fs to μs time range. Using different polymer/PCBM ratios we were able to distinguish between electron and hole motion dynamics.

EXPERIMENTAL SECTION

Methods. Integral mode photocurrent measurements were performed simultaneously with optical electric field probing (TREFISH) by measuring the voltage drop over the sample. The TREFISH technique was described in detail elsewhere;[13] a voltage drop occurs when displacement of photogenerated charge carriers compensates the applied electric field leading to a discharge of the capacitor-like sample. By adjusting the excitation intensity this voltage drop was set to be much smaller than the applied voltage. For an electric field homogeneously distributed over the active layer, the change of the voltage in the cell can be written as

$$\Delta U(t) = \frac{\Delta q(t)}{C} = \frac{1}{C}\int_0^t j(t')\,dt' \tag{1}$$

where C is the device capacitance and $\Delta q(t)$ is the charge transported by the photocurrent $j(t)$. The recorded photocurrent is proportional to the density of charge carriers and their drift speed:

$$j(t) = Aen(t)\frac{dl(t)}{dt} = Aen^0\left[1 - \frac{l(t)}{D}\right]\frac{dl(t)}{dt} \tag{2}$$

where A is the active area of the device and e is elementary charge, n^0 is the concentration of photogenerated charge carriers, $l(t)$ is the average carrier drift distance, and D is the device thickness. The term $1 - l(t)/D$ accounts for the carrier extraction. Assuming homogeneous charge carrier generation over the sample thickness, the total voltage drop at long times when all carriers are extracted equals $\Delta U(t > t_{ext}) = Aen^0D/2C$. Normalizing the time dependent voltage drop to the total voltage drop we obtain

$$\Delta U(t)_{norm} = \frac{2}{D^2}\int_0^t [D - l(t')]\frac{dl(t')}{dt'}\,dt' \tag{3}$$

Solving this equation we obtain the time dependence of the average drift distance and the carrier mobility, which in the case when the voltage drop is much smaller than the applied voltage equals

$$\mu(t) = \frac{D}{U_{appl}}\frac{dl(t)}{dt} \tag{4}$$

Samples. Fabrication of the inverted solar cells has been previously described elsewhere,[20] therefore only a brief account is given here. An aluminum electrode was evaporated onto a clean glass substrate followed by a titanium layer, which was then exposed to air for 12 h to form TiO_x. The active layer was spin-coated on top of the Al/TiO_x bilayer cathode from a solution of either the polyfluorene copolymer APFO3, $PC_{61}BM$, or the APFO3:$PC_{61}BM$ blends of composition ratios 2:1, 1:1, and 1:4 (by weight). The anode electrode, PEDOT-PSS PH1000, was deposited on top of the active layer followed by the encapsulation of the cell with a glass cover. The thickness of the active layer was ~100 nm, and the active area of the solar cells was ~5 mm^2.

Equipment. TREFISH measurements were performed by the pump−probe technique using femtosecond laser pulses. Ti-sapphire laser (Quantronix Integra-C) pulses of about 130 fs duration at 1 kHz were used to pump an optical parametric generator (TOPAS C, Light Conversion Ltd.), which generated excitation pulses at 550 nm (close to the absorption maximum of the polymer). The fundamental laser radiation at 800 nm was used as the probe to generate the second harmonic signal at 400 nm in the active material. The excitation power was set to 10 μW and 100 μW (corresponding to 2×10^{12} and 2×10^{13} photons/cm^2 per pulse) for the blends and neat polymer, respectively, causing small voltage drop in comparison with applied voltage. Reverse bias pulses of 10 μs duration synchronized with the laser pump pulses were applied to the devices through a load resistor, R_{load}, of 10 kΩ.

Pump−probe transient absorption measurements were performed in reflection mode in two different time windows, 100 fs to 10 ns and 10 ns to 10 μs. For the shorter time frame, pump pulses with 30 fs duration were produced by a 1 kHz non-collinear parametric amplifier at 550 nm (TOPAS-White, Light Conversion Ltd.). The long time frame measurements used 1 ns Nd:YAG laser (ACE) pump pulses at 532 nm. The probe pulses at 900 nm were generated by a non-collinear parametric amplifier (NOPA, Clark MXR, Inc.) for all measurements. The probe pulses were optically and electronically delayed for the shorter and longer time frames, respectively. Electromodulated differential absorption (EDA) measurements were performed in the nanosecond to microsecond time range by modifying the conventional TA measurements as described elsewhere.[21,22] In order to avoid carrier injection in these measurements, 500 μs electric field pulses with reverse bias polarity were applied for every second optical probe pulse. Pump pulses were applied for every probe pulse.

RESULTS AND DISCUSSION

Photovoltaic Performance. The photovoltaic performance of neat APFO3, neat $PC_{61}BM$, and APFO3:$PC_{61}BM$ devices under AM 1.5 solar illumination is characterized in Table 1. The charge generation efficiency in neat polymer films at low light intensities and in the absence of applied electric field is known to be very low,[23,24] in agreement with the solar cell performance measured for a neat APFO3 cell. The low current density and open circuit voltage of a neat $PC_{61}BM$ device are due to the very low absorbance of $PC_{61}BM$ in the visible spectral region and apparently low carrier generation efficiency leading to very low charge concentration. Open circuit voltage and fill factors of the different blending ratio devices are rather comparable, which according to Shuttle et al.[25] indicates that the built-in potential and charge

recombination are not drastically different for different blending compositions. It has been previously shown that geminate recombination is the dominating recombination process in APFO3:$PC_{61}BM$ films at low excitation fluencies, and that its rate is quite independent of the blending ratio.[26] The current density in the APFO3:$PC_{61}BM$ cells increases with the blending ratio in the order 2:1 < 1:1 < 1:4. Increase of the current density with relative $PC_{61}BM$ content has been attributed to better charge transport and reduced geminate recombination.[25] Combining the conclusions of refs 24 and 25 suggests that for APFO3:$PC_{61}BM$ improved charge transport with increasing PCBM content is the reason for increase of current density.

Electric Field Dynamics. More detailed insights into the underlying processes of the observed cell performance trends were obtained from the TREFISH and time-resolved photocurrent measurements described below. They enabled monitoring of the charge dynamics, from generation of bound charge pairs to their separation into mobile charges and finally extraction from the device. Figure 1 shows the electric field

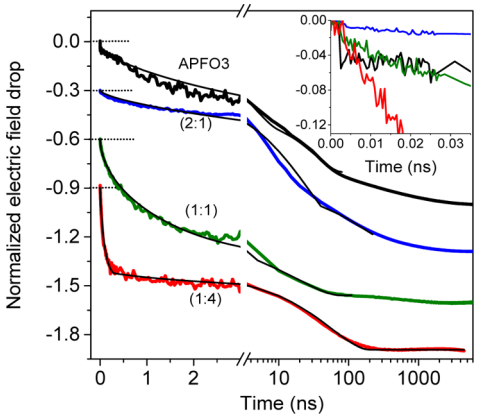

Figure 1. Normalized electric field kinetics of different blending ratio APFO3:$PC_{61}BM$ cells and of the neat APFO3 film (the curves are vertically shifted). The cells were reverse biased at 4 V. Thin black lines show modeled kinetics. The inset shows the initial part of the kinetics, revealing the exciton contribution in neat polymer film.

dynamics caused by the photocurrent in neat APFO3 and blend films monitored by TREFISH and TOF measurements. The voltage dynamics was normalized to the total voltage drop at long times when all charge carries were extracted. Assuming homogeneous charge generation across the thickness of the sample, the normalized voltage drop at some particular delay time approximately gives the fraction of extracted charge carriers at this time. It should be noted that much higher excitation fluence was used for the neat APFO3 film than for all the blends, because of lower carrier generation efficiency in neat APFO3. The electric field kinetics for the APFO3 device is similar to what has been observed previously for other conjugated polymers, and it has contributions from both excitons and mobile charges.[13] The exciton contribution is the very fast resolution-limited voltage drop at zero delay time (see inset in Figure 1) caused by the increased polarizability of the polymer chains in the excited state, which decays with the exciton lifetime of 175 ps.[27] The relative amplitude of the exciton contribution depends on the carrier generation efficiency. Given that the exciton contribution disappears on a sub-nanosecond time scale, the ensuing dynamics is mainly due to the motion of charges. Almost half of charge carriers are extracted during 3 ns, while extraction of the remaining half takes hundreds of nanoseconds. APFO3 is an ambipolar material with comparable steady-state electron and hole mobilities.[28] On the picosecond to sub-nanosecond time scale the THz conductivity is, however, dominated by hole mobility.[29] We therefore conclude that holes on the polymer significantly contribute to the photocurrent on this time scale, but we cannot decide on the exact ratio of electron and hole contribution, or their time dependencies.

No ultrafast exciton-related field response was observed for all blend devices (see inset in Figure 1), which confirms ultrafast exciton dissociation leading to efficient quenching of the polymer excited states and formation of randomly oriented charge pair (CP) states.[26] The absence of an ultrafast response also indicates that the polarizability of the CP state is relatively low, which may be interpreted as an indication of weak electron and hole delocalization in these blends.

The time evolution of the field strength in the 2:1 device is slightly slower than that in the neat APFO3 film both on sub-nanosecond and on sub-microsecond time scales, suggesting that both electron and hole mobilities are slightly lower. Decrease in the hole mobility may be expected because of the presence of the $PC_{61}BM$ domains, which perturb the hole motion. Electron transport properties in the blend are expected to be significantly different from those in pure polymer because electrons in the blend are transported over $PC_{61}BM$ domains. Electron mobility in $PC_{61}BM$ is quite high, on the order of 10^{-2}–10^{-1} $cm^2/(V\ s)$.[14−18] Simple estimates show that, with such a mobility, electron extraction should take place on a sub-nanosecond time scale, suggesting that the initial field dynamics should be attributed to electrons. However, the electron mobility in blends may be significantly lower, particularly at low $PC_{61}BM$ content when $PC_{61}BM$ molecules are dispersed in the polymer matrix or form small weakly percolating clusters. The percolation threshold depends on particle shape and appears at a concentration of about 20% $PC_{61}BM$.[8] Thus, the 33% $PC_{61}BM$ concentration in the 2:1 blend should be sufficient for percolation, but we cannot exclude the presence of isolated single $PC_{61}BM$ molecules, or weakly percolating clusters, which may act as electron traps reducing their mobility. For these reasons assignment of the time dependent field dynamics in the 2:1 device is not straightforward, but similarly to neat APFO3 polymer we suggest that the sub-nanosecond dynamics have significant contribution from hole extraction and that both holes and electrons contribute to the slower time scale.

The electric field kinetics is much faster in the 1:1 blend. Both $PC_{61}BM$ and polymer concentrations in this blend should be sufficient for extensive percolation between $PC_{61}BM$ and polymer domains, leading to high mobilities of both electrons and holes. Assuming that the hole mobility in the 1:1 blend decreases or remains similar to that in the 2:1 blend, the increase in the amplitude of the fast (<3 ns) field drop can be attributed to electrons. Almost all remaining charge carriers are extracted during less than 30 ns, indicating that the carrier extraction from this sample is close to balanced. The presence of a weak tens to hundreds of nanoseconds decay component indicates that some low concentration of trapped carriers are present in the 1:1 blend.

By further increasing the $PC_{61}BM$ concentration, large percolating $PC_{61}BM$ clusters are apparently formed and the electron mobility is expected to increase even more, approaching that observed in neat $PC_{61}BM$ films or crystals. The hole mobility, on the other hand, is expected to decrease.

dx.doi.org/10.1021/ja503301m | J. Am. Chem. Soc. 2014, 136, 11331−11338

The time evolution of the electric field strength in the 1:4 device is consistent with these expectations and shows a strong and rapid decay on the tens and hundreds of picoseconds time scale; a similar ultrafast electric field drop on the tens of picoseconds time scale was observed in neat $PC_{61}BM$.[19] Therefore, the extraction of about 50% of the charge carriers from the 1:4 blend within 1 ns can be related to the fast electron motion. The final carrier extraction from this blend is about twice slower than from the 1:1 blend, most likely as a consequence of lower hole mobility at the low (20%) polymer concentration.

In order to better characterize the electron and hole motion, we have modeled the field dynamics by approximating electron and hole mobilities by power-law functions $\mu(t) = \mu_0 t^{-\alpha}$ typical for carrier mobilities in disordered materials.[28] Thin lines in Figure 1 show the calculated electric field kinetics, and Figure 2

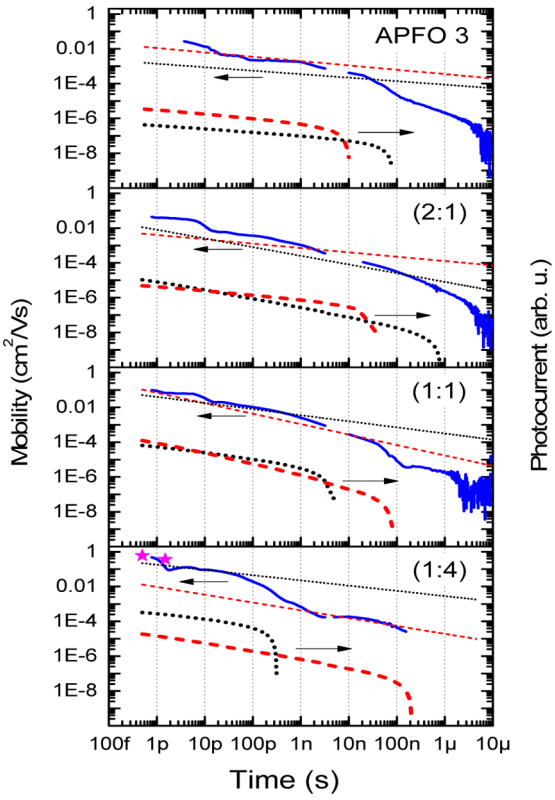

Figure 2. Experimentally measured average carrier mobility kinetics at 4 V applied voltage ($E \approx 4.8 \times 10^5$ V/cm) in neat APFO3 and in blends with different blending ratio (solid blue curves). Red stars show average carrier mobility of 1:4 device obtained from terahertz spectroscopy measurements.[25] Dashed lines show modeling results. Thin dashed black and red lines are electron and hole mobilities, respectively, while corresponding thick lines show electron and hole photocurrents.

presents photocurrents created by the two types of carriers as well as their calculated mobilities. Quite good agreement between experimental and calculated electric field kinetics validates the approximation of the carrier mobilities by power-law functions, although slightly lower modeled mobilities on the picosecond time scale (Figure 2) show that the power-law functions cannot describe the fine details of the initial mobility decay. The bending points of the current curves show the carrier extraction times. Electron and hole motion kinetics are clearly distinguishable for the 1:4 sample, where the electron extraction is more than 100 times faster than the hole extraction. We expect increase in the electron mobility and decrease in the hole mobility with increase of the $PC_{61}BM$ concentration. The modeling supports this expectation and allows us to attribute black curves to electrons and red curves to holes. This assignment is also in agreement with the carrier extraction in pure polymer: the hole extraction time is slightly shorter than in blends while electron extraction is several times slower, in agreement with 5 times higher steady state hole mobility.[28] Consequently the hole extraction slows down several times when $PC_{61}BM$ concentration increases. This weak dependence is a consequence of good percolation on long polymer chains, even at low polymer concentration. The electron extraction rate, on the contrary, changes by almost 4 orders of magnitude in going from the 2:1 to the 1:4 blend. Electron mobility at 80% $PC_{61}BM$ concentration in the 1:4 blend approaches that in pure $PC_{61}BM$, while at low concentration the electron mobility is apparently determined by spatial traps formed by single $PC_{61}BM$ molecules or weakly percolating domains, drastically reducing electron mobility. Additional reasons for the lower hole sensitivity to stoichiometry can probably be found in the smaller variation of hole mobility in polymer than of electron mobility in $PC_{61}BM$ upon going from isolated molecules to neat phase. In the amorphous APFO3 polymer, hole transport between chains is characterized by significant potential barriers implying that it does not increase as dramatically as the electron mobility going from single fullerene molecules to crystalline $PC_{61}BM$ domains.

The relatively slow, about 100 ns, hole extraction in the 1:4 blend is supported by the transient absorption (TA) kinetics shown in Figure 3a. At 900 nm the TA signal is due to absorption of holes,[3] which at zero applied field have fully decayed through recombination by 1 μs, while at applied voltage the decay was faster because of the hole extraction. TA kinetics during the initial 10 ns was independent of the applied voltage. According to the previous investigations the non-

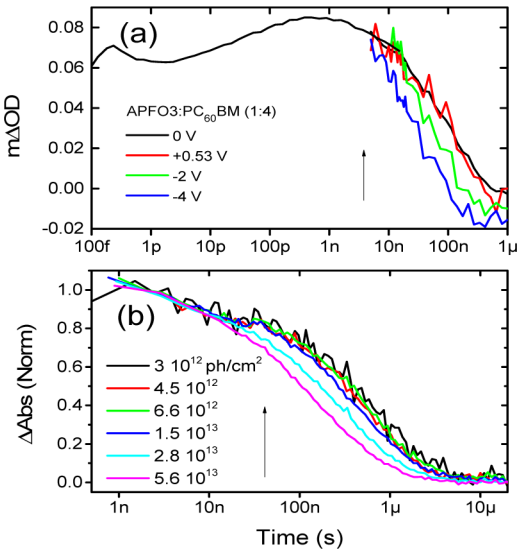

Figure 3. (a) Transient absorption of a 1:4 blend device at short circuit (0 V) condition (black) and at forward (+) and reverse (−) biases. The negative TA signal at long times under applied field is due to the extraction of equilibrium carriers. (b) Transient absorption of 1:1 blend at different excitation photon densities. Excitation was performed at 532 nm by 1 ns duration pulses.

dx.doi.org/10.1021/ja503301m | J. Am. Chem. Soc. 2014, 136, 11331−11338

geminate recombination in APFO3:$PC_{61}BM$ films is negligible on a picosecond to nanosecond time scale, below an excitation intensity of about 10^{13} photons/cm^2/pulse.[25] We have additionally addressed the intensity dependence of the recombination dynamic on a longer time scale (see Figure 3b). The increase of the recombination rate due to non-geminate recombination becomes apparent only at 1.5×10^{13} photon/cm^2, i.e., at an excitation intensity 1 order of magnitude higher than used in the present investigations. The influence of the nongeminate recombination at applied voltage is in addition expected to be lower than under the field-free conditions of Figure 3b, because of faster carrier extractions. Thus, we can safely neglect nongeminate recombination in our data analysis for the present materials, under the experimental conditions used. Consequently the hole decay at zero applied field should be attributed to the geminate recombination. The carrier decay time decreases to tens of nanoseconds at 4 V applied voltage (Figure 3b) as a result of charge extraction, in perfect agreement with the charge extraction kinetics shown in Figure 1. This confirms that the slow charge extraction phase on the tens of nanoseconds time scale in the electric field kinetics of the 1:4 blend device (Figure 2) is due to hole extraction.

It should be pointed out that TREFISH measurements require an applied voltage corresponding to an external electric field several times higher than that in an operating solar cell. The stronger field leads to faster charge separation, drift, and extraction, implying that absolute durations of these events should not be taken as characterizing processes in operating solar cells. Nevertheless, the observed trends and material dependencies contain relevant information about the functioning of devices. Figure 4 shows the voltage dynamics at longer

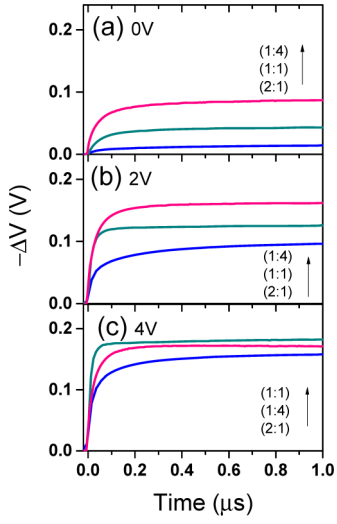

Figure 4. Transient voltage kinetics on different stoichiometry devices at different applied voltages. The transient voltage was corrected for the equal number of absorbed photons.

times measured at different applied voltages by an oscilloscope. The voltage drop increases with the applied voltage, and the increase is particularly strong for the 2:1 device, indicating that efficient carrier generation or extraction requires strong electric field. In contrast, carrier extraction from the 1:4 device at 4 V is only about twice as large as at build-in electric field. The voltage kinetics becomes progressively faster at higher voltages, and this is particularly clear in the case of the 1:1 sample. The other two samples show much weaker dependences of the transient kinetics on the applied voltage. This can be interpreted as an indication that the carrier extraction in the 2:1 device on the tens and hundreds of nanoseconds time scale is governed by thermal release of electrons from traps, in agreement with the conclusion above that a fraction of electrons in the 2:1 sample and holes in the 1:4 sample are trapped in weakly percolating $PC_{61}BM$ or polymer clusters. Only in case of the 1:1 sample, where percolative motion of both carrier types is optimized (for this material), the extraction rate significantly increases with the applied voltage, which is expected if carrier extraction is limited by mobility. Figure 5 summarizes the carrier extraction results

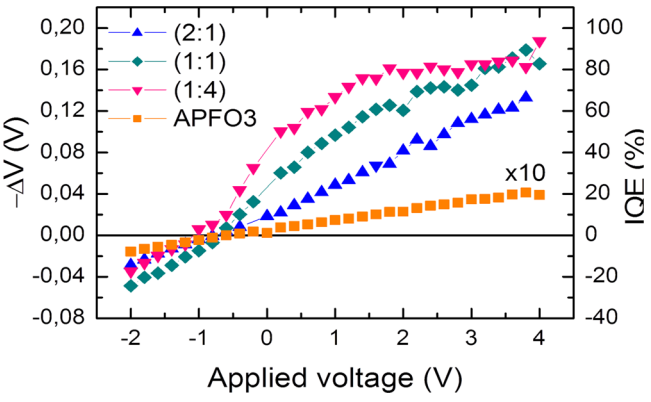

Figure 5. Total voltage drop corrected for the number of absorbed photons as a function of applied voltage. The right axes shows the calculated internal quantum efficiency (IQE).

from all samples presenting dependences of the internal quantum efficiency (IQE) on applied voltage measured at the same excitation conditions. The IQE at 550 nm was evaluated as the number of generated charge carriers determined from the total voltage drop at long time divided by the number of absorbed light quanta. Carrier extraction from the 1:4 sample saturates at 2 V suggesting that the majority of excitons split into charge carriers, which are efficiently extracted. For the 1:1 and particularly the 2:1 samples, on the other hand, higher applied voltages are required for efficient carrier extraction.

The voltage drop at long times at 0 V applied voltage is expected to be proportional to the short circuit current in an operating solar cell. The short circuit current under steady state excitation (see Table 1) in the 2:1, 1:1, and 1:4 devices (normalized to the signal recorded for the 2:1 device) increases as 1, 1.86, and 2.15 whereas the relative voltage drop (from Figure 4) increases somewhat more, 1, 2.3, and 4.1. The discrepancy is probably mainly caused by different sample excitation conditions. For pulsed excitation, not all electrons are extracted from the samples with low $PC_{61}BM$ concentration during the measurement time of several microseconds, because some of them remain trapped on single $PC_{61}BM$ molecules or in weakly percolating domains. For CW excitation a stationary state with filled trapping sites is established and their influence is therefore reduced.

Carrier Mobility: TREFISH vs THz. The time dependent carrier mobility, averaged over electrons and holes, can be also obtained directly (see Experimental Section) from the TREFISH and transient photocurrent measurements. Figure 2 shows the experimental averaged mobilities. At short times the averaged mobilities correspond to the mean values between electron and hole mobilities. At long times, when fast carriers

dx.doi.org/10.1021/ja503301m | J. Am. Chem. Soc. 2014, 136, 11331−11338

are already extracted, the average mobilities approach those of slower carriers. The averaged carrier mobilities in all samples decrease by about 4 orders of magnitude during approximately ten nanoseconds to reach long time values similar to those previously reported in the literature.[29,30] It should be noted that the carrier mobility dynamics is expected to be free of influence of changing charge carrier concentration. This is because geminate recombination can be ruled out at strong electric field, while nongeminate recombination, as was discussed, is not substantial at our excitation intensities.

Carrier mobility and its time dependence can also be obtained from time-resolved THz conductivity measurements.[29−32] For APFO3/$PC_{61}BM$ blends such measurements resulted in a mobility for the 1:4 blend remarkably similar to the averaged mobility obtained here with the TREFISH technique (Figure 5) at early delay times around 1 ps. However, from the measurements of blends with varying polymer chain lengths (APFO3 monomer to various molecular weight polymers) it was concluded that THz mobility of holes on the polymer chain is approximately five times higher (on the few-picoseconds time scale) than of electrons in $PC_{61}BM$.[29] This discrepancy in relative electron/hole mobility obtained by the two techniques can be understood as a difference in how they "sense" the carrier mobility. It was concluded that at a frequency of ∼1 THz this spectroscopy probes the motion of charges over a distance of ∼2−10 nm, corresponding to only a few polymer units.[33] Thus, TREFISH and THz seem to probe somewhat different aspects of charge mobility: THz conductivity measures charge mobility over short nanometer distances, whereas TREFISH measurements, based on the drift of charges, can be expected to measure mobility over longer distances. This implies that the TREFISH mobility is probably more closely related to the extraction kinetics, at least on longer time scale. In a way, THz photoconductivity measurements reflect mainly an ability of charges to move, whereas TREFISH better reflects transport of charge carriers. Yet, on the shorter time and distance scale, both THz and TREFISH mobilities may be closely correlated. It is important to note that precisely this time scale is of critical importance for separation of charges initially generated at the place of photon absorption, to distances where their Coulomb attraction is overcome. In any case, both TREFISH and THz measurements for the 1:4 blend in Figure 2 show that the carrier mobility is high irrespective of the method of measurement. Figure 2 also shows that the carrier mobility is strongly time dependent, as expected, and shown before to be a result of relaxation in the density of states.[6,34] However, considering that the measured mobility has contributions from both electron and hole mobilities, and that these most likely have different time dependencies, only modeling helps to determine the ratio of electron and hole mobility at an arbitrary time.

By correlating TREFISH mobility and extraction kinetics for the 1:4 blend we could conclude that the early time mobility of ∼1 $cm^2/(V\,s)$ (Figure 2) can be mainly correlated to electrons. At times >1 ns in this blend most of the electrons are extracted (Figure 1), implying that the measured TREFISH mobility (10^{-3} $cm^2/(V\,s)$) beyond this time can be attributed to holes on the polymer. We concluded above that the hole mobility is relatively weakly dependent on the polymer:fullerene blending ratio. This is expected to be particularly true at short times, when intrachain mobility dominates. The hole mobility decreases by a factor of ∼100 over the first nanosecond. This is a somewhat stronger time dependence of hole mobility in APFO3 than suggested by time-resolved THz measurements,[29,30] but is in line with the discussion above of differences in how THz and TREFISH measurements probe carrier mobility.

Implications for the charge carrier generation mechanism and solar cell performance:

1. The saturation of IQE at 2 V in the 1:4 sample with 80% $PC_{61}BM$ (Figure 5) shows that both generation and extraction of free charges saturate above this value, suggesting that both of these processes approach 100% efficiency. The fact that the carrier extraction efficiency in cells with lower $PC_{61}BM$ concentration is several times lower and shows no saturation indicates that at least one of these processes requires much stronger electric field to reach high efficiency. Since nongeminate recombination in our experiments is negligible, the voltage dependence of extracted charge is determined by the generation efficiency of free charges. Thus, for the nonoptimal (2:1 and 1:1) blends an external electric field is required to separate electrons and holes and convert them into free mobile charges that can be extracted.
2. For effective free carrier generation and extraction, high carrier mobility is essential[35,36] although in the literature there is no agreement on which of electron[37−39] and hole[40,41] mobility is higher and plays the more important role. Our results provide a quantitative characterization of both mobilities, show that the electron mobility plays a crucial role in this type of polymer/fullerene blend, and suggest that this could be a general feature of all polymer/fullerene blends as the fullerene part of the blends is the same. The extracted charge and the solar cell efficiency increase with $PC_{61}BM$ concentration when the electron mobility increases.[37−42] Balanced charge motion, when both electrons and holes have approximately equal mobility, does not necessarily ensure the best cell performance. High mobility over large distances of one type of charge carrier is more important for efficient solar cell operation. As we have recently demonstrated, the initial charge separation at weak electric field is mostly governed by diffusion,[6] directly proportional to carrier mobility. Thus, at high $PC_{61}BM$ concentration, electrons diffuse sufficiently far from the hole to avoid fast geminate recombination, and even a weak electric field is sufficient to prevent geminate recombination at long times. Access to delocalized π electron states in ordered regions of the fullerene acceptor material within 40 fs after light absorption in an OPV model system[3] could be another aspect of these observations.
3. In the case of low $PC_{61}BM$ concentration, fast electron motion is either restricted to small $PC_{61}BM$ domains or not possible at all if the CP state is formed on a single $PC_{61}BM$ molecule. If the electron localization domain is smaller than the Coulomb radius (10−15 nm), then carrier separation depends on motion of the hole. Apparently the relatively restricted slow hole motion in APFO3 is not sufficient to separate the charge carriers before their geminate recombination. By applying a strong external electric field to the low $PC_{61}BM$ concentration cells the IQE approaches that of the 1:4 device (Figure 4). This can be understood as a result of a combined action of restricted (and high) hole diffusion

and electric field induced drift over polymer segments separated by potential barriers.

4. Fast and balanced carrier extraction from the 1:1 device does not ensure its best solar energy conversion, which shows that it is not the carrier extraction which limits its performance efficiency. The generation efficiency of mobile charges at low electric field strongly increases with the $PC_{61}BM$ concentration and correlates with the carrier separation rate illustrated by TREFISH kinetics. Since fast carrier separation in blends with high $PC_{61}BM$ concentration mainly relies on the electron mobility, we conclude that fast electron motion is essential for efficient charge carrier separation preventing their geminate recombination ensuring the best performance of the 1:4 solar cell despite slow hole extraction.

CONCLUSIONS

Charge carrier motion in APFO3:$PC_{61}BM$ blends has been investigated by means of sub-picosecond TREFISH measurements of the internal electric field, combined with conventional transient photocurrent measurements. Blends of different stoichiometries were studied in order to disentangle electron and hole transport kinetics. Although the measurements were performed at stronger electric field than in operating solar cells, the carrier motion dynamics is expected to be qualitatively similar. The motion dynamics was found to depend crucially on the polymer:$PC_{61}BM$ ratio of the materials. For the sample with 80% $PC_{61}BM$, most of the electrons are extracted within less than 100 ps at 4 V applied voltage; for a low-$PC_{61}BM$ sample (33% $PC_{61}BM$), extraction is much slower, tens and hundreds of nanoseconds. Extraction of holes is less dependent on the polymer:$PC_{61}BM$ ratio; hole extraction changes from several tens of nanoseconds to more than 100 ns when the polymer content decreases from 67% to 20%. IQE and solar cell efficiency for polymer:fullerene cells in general, and the APFO3:$PC_{61}BM$ devices studied here in particular, are strongly dependent on fullerene concentration; fullerene concentrations of $\geq$50% (w/w) are required for the best solar cell performance. Our results now show that this fact can be traced to the very strong dependence of electron mobility in the fullerene phase on the polymer:fullerene ratio, giving rise to a variation of extraction times by a factor of more than 1000 when the fullerene content is varied from 33% to 80%. At the same time the hole mobility changes much less (approximately ten times), making the precise nature of the polymer phase and its hole mobility less critical for the solar cell performance. We conclude that fast electron motion between fullerene molecules is essential for solar cells enabling efficient separation of geminate charge pairs in low electric field in devices. Carrier separation via hole motion when electrons are immobile is much slower and requires strong electric field not present in operating solar cells. It is worth noting that we have recently observed similar electron and hole mobility dependences on the blending ratio in other efficient blends of fullerenes with polymers and small molecules. This also explains why different polymer and small molecule donors show similar performance in solar cells based on bulk heterojunctions with fullerene derivatives.

AUTHOR INFORMATION

Corresponding Author

*Villy.Sundstrom@chemphys.lu.se

Author Contributions

The manuscript was written through contributions of all authors.

Notes

The authors declare no competing financial interest.

ACKNOWLEDGMENTS

We thank the Swedish and European Research Councils (226136-VISCHEM), Swedish Energy Agency and Knut & Alice Wallenberg Foundation.

REFERENCES

(1) Green, M. A.; Emery, K.; Hishikawa, Y.; Warta, W.; Dunlop, E. D. *Prog. Photovoltaics: Res. Appl.* **2013**, *21*, 1.

(2) You, J.; Dou, L.; Yoshimura, K.; Kato, T.; Ohya, K.; Moriarty, T.; Emery, K.; Chen, C.-C.; Gao, J.; Li, G.; Yang, Y. *Nat. Commun.* **2013**, *4*, 1446.

(3) Gélinas, S.; Rao, A.; Kumar, A.; Smith, S. L.; Chin, A. W.; Clark, J.; van der Poll, T. S.; Bazan, G. C.; Friend, R. H. *Science* **2014**, *343*, 512.

(4) Strobel, T.; Deibel, C.; Dyakonov, V. *Phys. Rev. Lett.* **2010**, *105*, 266602.

(5) Bakulin, A. A.; Rao, A.; Pavelyev, V. G.; van Loosdrecht, P. H. M.; Pshenichnikov, M. S.; Niedzialek, D.; Cornil, J.; Beljonne, D.; Friend, R. H. *Science* **2012**, *335*, 1340.

(6) Vithanage, D. A.; Devižis, A.; Abramavičius, V.; Infahsaeng, Y.; Abramavičius, D.; Mackenzie, R. C. I.; Keivanidis, P. E.; Yartsev, A.; Hertel, D.; Nelson, J.; Sundström, V.; Gulbinas, V. *Nat. Commun.* **2013**, *4*, 2334.

(7) Abramavičius, V.; Amarasinghe Vithanage, D.; Devižis, A.; Infahsaeng, Y.; Bruno, A.; Foster, S.; Keivanidis, P. E.; Abramavičius, D.; Nelson, J.; Yartsev, A.; Sundström, V.; Gulbinas, V. *Phys. Chem. Chem. Phys.* **2014**, *16*, 2686.

(8) Bartelt, J. A.; Beiley, Z. M.; Hoke, E. T.; Mateker, W. R.; Douglas, J. D.; Collins, B. A.; Tumbleston, J. R.; Graham, K. R.; Amassian, A.; Ade, H.; Fréchet, J. M. J.; Toney, M. F.; McGehee, M. D. *Adv. Energy Mater.* **2013**, *3*, 364.

(9) Geiser, A.; Fan, B.; Benmansour, H.; Castro, F.; Heier, J.; Keller, B.; Mayerhofer, K. E.; Nüesch, F.; Hany, R. *Sol. Energy Mater. Sol. Cells* **2008**, *92*, 464.

(10) Howard, I. A.; Mauer, R.; Meister, M.; Laquai, F. *J. Am. Chem. Soc.* **2010**, *132*, 14866.

(11) Zhang, F.; Jespersen, K. G.; Björström, C.; Svensson, M.; Andersson, M. R.; Sundström, V.; Magnusson, K.; Moons, E.; Yartsev, A.; Inganäs, O. *Adv. Funct. Mater.* **2006**, *16*, 667.

(12) Prins, P.; Grozema, F.; Schins, J.; Patil, S.; Scherf, U.; Siebbeles, L. *Phys. Rev. Lett.* **2006**, *96*, 146601.

(13) Devižis, A.; Serbenta, A.; Meerholz, K.; Hertel, D.; Gulbinas, V. *Phys. Rev. Lett.* **2009**, *103*, 027404.

(14) Anthopoulos, T. D.; Tanase, C.; Setayesh, S.; Meijer, E. J.; Hummelen, J. C.; Blom, P. W. M.; de Leeuw, D. M. *Adv. Mater.* **2004**, *16*, 2174.

(15) Waldauf, C.; Schilinsky, P.; Perisutti, M.; Hauch, J.; Brabec, C. J. *Adv. Mater.* **2003**, *15*, 2084.

(16) Meijer, E. J.; de Leeuw, D. M.; Setayesh, S.; van Veenendaal, E.; Huisman, B. H.; Blom, P. W. M.; Hummelen, J. C.; Scherf, U.; Kadam, J.; Klapwijk, T. M. *Nat. Mater.* **2003**, *2*, 678.

(17) Singh, T. B.; Marjanović, N.; Stadler, P.; Auinger, M.; Matt, G. J.; Günes, S.; Sariciftci, N. S.; Schwödiauer, R.; Bauer, S. *J. Appl. Phys.* **2005**, *97*, 083714.

(18) Tuladhar, S. M.; Poplavskyy, D.; Choulis, S. A.; Durrant, J. R.; Bradley, D. D. C.; Nelson, J. *Adv. Funct. Mater.* **2005**, *15*, 1171.

(19) Cabanillas-Gonzalez, J.; Virgili, T.; Gambetta, A.; Lanzani, G.; Anthopoulos, T. D.; de Leeuw, D. M. *Phys. Rev. Lett.* **2006**, *96*, 106601.

(20) Tang, Z.; Andersson, L. M.; George, Z.; Vandewal, K.; Tvingstedt, K.; Heriksson, P.; Kroon, R.; Andersson, M. R.; Inganäs, O. *Adv. Mater.* **2012**, *24*, 554.

(21) Gulbinas, V.; Zaushitsyn, Y.; Sundström, V.; Hertel, D.; Bässler, H.; Yartsev, A. *Phys. Rev. Lett.* **2002**, *89*, 107401.
(22) Zaushitsyn, Y.; Gulbinas, V.; Zigmantas, D.; Zhang, F.; Inganäs, O.; Sundström, V.; Yartsev, A. *Phys. Rev. B* **2004**, *70*, 075202.
(23) Scheblykin, I. G.; Yartsev, A.; Pullerits, T.; Gulbinas, V.; Sundström, V. *J. Phys. Chem. B* **2007**, *111*, 6303.
(24) Arkhipov, V.; Bässler, H.; Emelyanova, E.; Hertel, D.; Gulbinas, V.; Rothberg, L. *Macromol. Symp.* **2004**, *212*, 13.
(25) Shuttle, C.; Hamilton, R.; O'Regan, B. C.; Nelson, J.; Durrant, J. R. *Proc. Natl. Acad. Sci. U.S.A.* **2010**, *107*, 16448.
(26) De, S.; Pascher, T.; Maiti, M.; Jespersen, K. G.; Kesti, T.; Zhang, F.; Inganäs, O.; Yartsev, A.; Sundström, V. *J. Am. Chem. Soc.* **2007**, *129*, 8466.
(27) De, S.; Kesti, T.; Maiti, M.; Zhang, F.; Inganäs, O.; Yartsev, A.; Pascher, T.; Sundström, V. *Chem. Phys.* **2008**, *350*, 14.
(28) Schubert, M.; Preis, E.; Blakesley, J.; Pingel, P.; Scherf, U.; Neher, D. *Phys. Rev. B* **2013**, *87*, 024203.
(29) Ponseca, C. S.; Nemec, H.; Vukmirovic, N.; Fusco, S.; Wang, E.; Andersson, M. R.; Chabera, P.; Yartsev, A.; Sundstro, V. *J. Phys. Chem. Lett.* **2012**, *3*, 2442.
(30) Ponseca, C. S.; Yartsev, A.; Wang, E.; Andersson, M. R.; Vithanage, D.; Sundström, V. *J. Am. Chem. Soc.* **2012**, *134*, 11836.
(31) Esenturk, O.; Melinger, J. S.; Heilweil, E. J. *J. Appl. Phys.* **2008**, *103*, 023102.
(32) Cunningham, P. D.; Hayden, L. M. *J. Phys. Chem. C* **2008**, *112*, 7928.
(33) Vukmirović, N.; Ponseca, C. S.; Němec, H.; Yartsev, A.; Sundström, V. *J. Phys. Chem. C* **2012**, *116*, 19665.
(34) Jones, M. L.; Chakrabarti, B.; Groves, C. *J. Phys. Chem. C* **2014**, *118*, 85.
(35) Pal, S. K.; Kesti, T.; Maiti, M.; Zhang, F.; Inganäs, O.; Hellström, S.; Andersson, M. R.; Oswald, F.; Langa, F.; Osterman, T.; Pascher, T.; Yartsev, A.; Sundström, V. *J. Am. Chem. Soc.* **2010**, *132*, 12440.
(36) Vithanage, D. A.; Wang, E.; Wang, Z.; Ma, F.; Inganäs, O.; Andersson, M. R.; Yartsev, A.; Sundström, V.; Pascher, T. *Adv. Energy Mater.* **2014**, 1301706.
(37) van Duren, J. K. J.; Yang, X.; Loos, J.; Bulle-Lieuwma, C. W. T.; Sieval, A. B.; Hummelen, J. C.; Janssen, R. A. J. *Adv. Funct. Mater.* **2004**, *14*, 425.
(38) Mihailetchi, V. D.; van Duren, J. K. J.; Blom, P. W. M.; Hummelen, J. C.; Janssen, R. A. J.; Kroon, J. M.; Rispens, M. T.; Verhees, W. J. H.; Wienk, M. M. *Adv. Funct. Mater.* **2003**, *13*, 43.
(39) Veldman, D.; Ipek, O.; Meskers, S. C. J.; Sweelssen, J.; Koetse, M. M.; Veenstra, S. C.; Kroon, J. M.; van Bavel, S. S.; Loos, J.; Janssen, R. A. J. *J. Am. Chem. Soc.* **2008**, *130*, 7721.
(40) Andersson, L. M.; Zhang, F.; Inganäs, O. *Appl. Phys. Lett.* **2007**, *91*, 071108.
(41) Savenije, T.; Kroeze, J.; Wienk, M.; Kroon, J.; Warman, J. *Phys. Rev. B* **2004**, *69*, 155205.
(42) Andersson, L. M.; Inganäs, O. *Appl. Phys. Lett.* **2006**, *88*, 082103.

■ NOTE ADDED AFTER ASAP PUBLICATION

The descriptions of electron and hole mobilities (Table 1 and power-law functions in section Electron Field Dynamics) have been corrected. The revised version was re-posted on July 29, 2014.